

BAND TAIL STATES IN MICROCRYSTALLINE SILICON SOLAR CELLS PROBED BY PHOTOLUMINESCENCE AND OPEN CIRCUIT VOLTAGE

R. Carius^{a*}, T. Merdzhanova^{a,b}, S. Klein^a, F. Finger^a

^aInstitut für Photovoltaik, Forschungszentrum Jülich GmbH, 52425 Jülich, Germany

^bCentral Laboratory for Solar Energy and New Energy Sources, Bulgarian Academy of Sciences, 72 Tzarigradsko Chaussee, 1784 Sofia, Bulgaria

Thin film p-i-n microcrystalline silicon ($\mu\text{c-Si:H}$) solar cells were studied by photoluminescence (PL) spectroscopy and open circuit voltage, V_{oc} . By this means, the cause of the commonly observed increase of V_{oc} when the silane concentration in the gas phase for the preparation of the intrinsic absorber layers is raised is addressed. The hot wire chemical vapour deposition (HW-CVD) technique was used for the preparation of films and intrinsic absorber layers of solar cells with efficiencies higher than 9%. By monitoring V_{oc} and the PL energy, E_{PL} , as a function of temperature, information on the photogenerated carrier distributions and the splitting of the quasi-Fermi energies was gained and the effect of states in the gap was studied by comparison with results from a crystalline p-i-n diode. An increase of E_{PL} and V_{oc} for increasing SC and decreasing temperature is attributed to the shift of the excess carrier distributions to higher energies. It is proposed that this shift is limited by band tail states. It is proposed that increasing SC leads to a reduction of the density of band tail states, due to structural relaxation of the $\mu\text{c-Si:H}$ network by the presence of hydrogen or hydrogenated amorphous silicon.

(Received December 9, 2004; accepted January 26, 2005)

Keywords: Photoluminescence, Open circuit voltage, Solar cells, Microcrystalline silicon

1. Introduction

Microcrystalline silicon ($\mu\text{c-Si:H}$) thin films have attracted great interest because of their potential applications in thin film electronics and thin film solar cells. High quality $\mu\text{c-Si:H}$ can be prepared at low substrate temperatures on a large variety of substrate materials such as glass, stainless steel and even plastics. A significant advantage is the compatibility of the deposition techniques with the quite mature amorphous silicon technology. The films are usually prepared from silane highly diluted in hydrogen. By increasing the silane concentration (SC) in the hydrogen gas, the microstructure of the material can be changed from highly crystalline to amorphous [1]. Previous studies on $\mu\text{c-Si:H}$ solar cells have shown an increased open circuit voltage (V_{oc}) when the intrinsic (i-) layers were prepared with increasing SC, irrespective of the deposition method, e.g. plasma enhanced chemical vapour deposition (PE-CVD) [2-4] or hot wire chemical vapour deposition (HW-CVD) [5]. In particular, $\mu\text{c-Si:H}$ solar cells with i-layers deposited near the transition from crystalline to amorphous growth exhibit the best performance [2,3,5]. Studies of the photo- and dark conductivity on undoped material showed a continuous decrease with increasing SC [2]. It was also found that the PL band, which is located below the band gap of crystalline silicon, shifts to higher energies with increasing SC, i.e. with decreasing crystalline volume fraction [6-11]. This featureless band is much broader than the luminescence spectra observed in high quality crystalline silicon, and is about half the width of the photoluminescence band found in a-Si:H, e.g. [8,11,12]. The origin of this PL band is not yet clear. Radiative recombination at defects in the crystalline phase, transitions

* Corresponding author: r.carius@fz-juelich.de

between states in the grain boundary region or transitions between localized tail states similar to the case of amorphous silicon have been discussed [6-12]. However, there is evidence that the recombination process involves localized states and the recombination processes show similarities with those found in a-Si:H. Therefore, we assume that the PL originates from transitions between localized band tail states similar to those in a-Si:H [7,13].

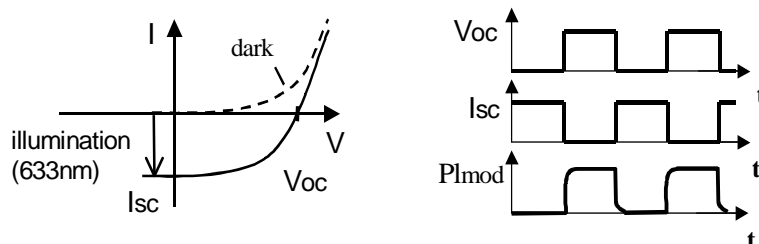


Fig. 1. Schematic representation of the current-voltage characteristics of a p-i-n solar cell in the dark and under illumination (left); the time sequence of the modulation technique, together with the expected signals to be measured (right).

Here, a systematic study of the influence of the SC (respectively the crystalline volume fraction) on the PL properties and V_{oc} of very high quality $\mu\text{c-Si:H}$ solar cells is provided, in order to obtain more information on the density and distribution of the tail states and its influence on V_{oc} in this solar cells. The emphasis is on the relationship between V_{oc} , i.e. the splitting of the quasi-Fermi energies and PL peak energy, i.e. the carrier distributions in the band tails.

2. Experimental details

Raman measurements in a back-scattering geometry were performed with the 488nm line of an Ar-ion laser or the 647 nm line of a Krypton laser for excitation. Details of the set-up and the data evaluation have been published elsewhere [1,5]. Photoluminescence (PL) spectra were measured with a Fourier transform (FT) spectrometer (Bruker FS66v) and detected either with a LN₂ cooled Ge or an InAs detector. For the measurements, the samples were mounted in a continuous flow helium cryostat, providing temperatures from 10 to 300 K. Measurements on solar cells were performed using a modulation technique, in order to eliminate spurious PL signals from the glass, the transparent conductive oxide (TCO) and the p-layer, and to detect the relevant carriers involved in the photovoltaic process, as explained below. Here, the 632.8 nm line of a He-Ne laser was used to provide homogeneous generation throughout the samples. The applied photon flux of about $10^{18} \text{ cm}^{-2} \text{ s}^{-1}$ led to a 10 times higher short-circuit current density as compared to AM 1.5 illumination. An external voltage was applied to the solar cells and switched from 0 V to V_{oc} (20 Hz, rectangular shape, 50% duty cycle) using a HP 8116A pulse generator.

Fig. 1(a) shows the I-V characteristics of a solar cell in the dark and under illumination, and the two important parameters short circuit current, I_{sc} , and open circuit voltage, V_{oc} , are indicated. The time sequence of the measurement, together with the expected signals to be measured is schematically shown in Fig. 1(b). At V_{oc} (i.e. $I = 0$) where full carrier recombination and no extraction from the i-layer occurs, the maximum PL signal will be obtained. The minimum PL signal will be obtained at I_{sc} - where full carrier extraction and no recombination is expected in the ideal case. With this technique, only those carriers relevant to the photovoltaic process are probed, and spurious signals from the doped layers, glass substrate, etc. are suppressed. The change of the PL signal upon changing the applied voltage from 0 V to V_{oc} was detected by a lock-in technique, while the FT-spectrometer was operated in step-scan mode. I_{sc} was monitored with a digital oscilloscope (Le Croy 9400). The contact area was typically 1 mm^2 . A Keithley 2400 source meter was used for the V_{oc} and I_{sc} measurements, under steady state conditions. The investigated $\mu\text{c-Si:H}$ solar cells were prepared at a substrate temperature of $T_s=185 \text{ }^\circ\text{C}$ in a p-i-n deposition sequence on textured ZnO substrates with a ZnO/Ag back reflector. HW-CVD at a deposition pressure (P_d) of 3.5 - 5 Pa was used to deposit the intrinsic layers. The microstructure of the i-layers with thickness between 0.85 and $1.3 \text{ }\mu\text{m}$ was modified by varying the dilution of the silane process gas in hydrogen ($SC=[\text{SiH}_4]/[\text{SiH}_4+\text{H}_2]$), keeping the conditions for all other layers constant. Details of the

deposition parameters are published elsewhere [5,14]. A commercially available p-i-n diode (Hamamatsu S1190) of active diameter 1 mm was used as a reference.

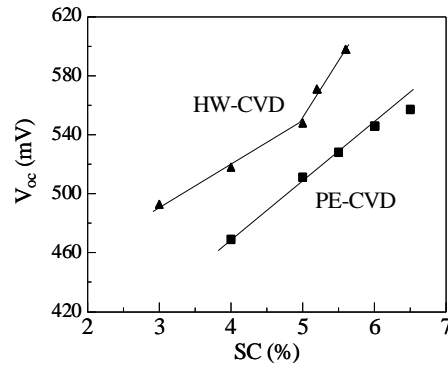


Fig. 2. Open circuit voltage V_{oc} at 300K as a function of the silane concentration in the gas phase for two series of solar cells deposited by PE-CVD and HW-CVD.

3. Results

In Fig. 2, V_{oc} is plotted as a function of the silane concentration used for the i-layer preparation, for two series of solar cells prepared by HW-CVD and PE-CVD [2, 14]. The data points for the highest SC values refer to those that still provide cells with good extraction properties. A still higher SC leads to even higher V_{oc} , but also to a degradation of the solar cell parameters (low I_{sc} and fill factor). With increasing SC, V_{oc} increases almost linearly for the PE-CVD series, by about 100 mV. For the HW-CVD cells, the V_{oc} is higher and the increase seems to be steeper at higher SC. However, the overall change is very similar and is in line with observations from other series and from other groups.

Fig. 3, the maximum of the photoluminescence energy (E_{PL}) measured in the conventional way at 10 K is plotted as a function of SC for two series of films (full symbols) prepared by PECVD and HW-CVD at different substrate temperatures. The data suggest that E_{PL} as a function of SC exhibits a similar trend to that as a function of V_{oc} , as shown in Fig. 1, although the magnitude of the changes is different. A more detailed investigation of several sample series made by HW-CVD or PE-CVD reveals a common trend, i.e. at low SC the increase of E_{PL} is less pronounced (or even constant) but at high SC, E_{PL} changes more rapidly. In addition to the data for the films, results for the intrinsic layer of the HW-CVD solar cells are shown. They exhibit the same trend as observed for the films.

In Fig. 4, PL spectra obtained by the modulation technique on solar cells with different silane concentrations (3 - 5.6%), measured at 150 K, are shown. For the lowest SC, the PL spectra reveal a broad emission band with a maximum at about 0.86 eV ($\mu\text{c-Si}$ -band) and a half-width of about 0.14 eV, attributed to the microcrystalline phase.

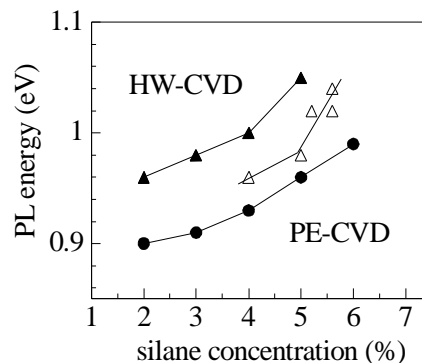


Fig. 3. Photoluminescence peak energy E_{PL} measured at 10 K as a function of the silane concentration for two series of films deposited by PE-CVD and HW-CVD and for the intrinsic layers of the solar cells investigated in this study.

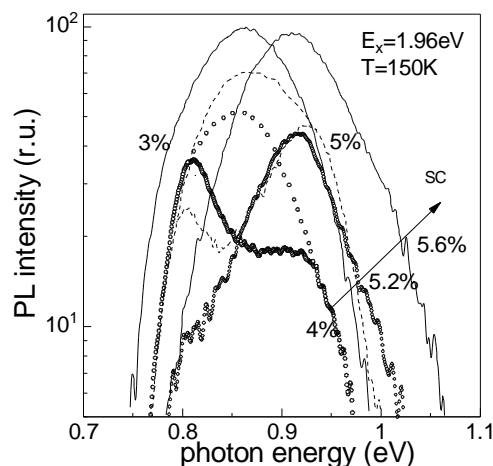


Fig. 4. Modulated PL spectra of solar cells with i-layers prepared with different SC by HW-CVD measured at 150K. Note the logarithmic intensity scale. The interference fringes are tentatively corrected for the solar cells with 4% and 5% SC.

The luminescence energy is similar to that observed in a conventional photoluminescence measurement on films at the same temperature. To demonstrate the shift of the $\mu\text{-Si}$ -band towards higher energies with increasing SC (up to 0.91 eV), and the absence of any contribution at 1.35 eV originating from an amorphous phase, a logarithmic intensity scale was chosen. Interference fringes modify the shape of the PL spectra for solar cells with SC between 4% and 5.2%. The indicated open circles and dashed line refer to tentatively corrected spectra. The PL intensity (given in relative units) and the width of the PL band are very similar for all solar cells, and thus the quantum efficiency of the PL does not change significantly.

In Fig. 5, E_{PL} as a function of the silane concentration is shown for modulated spectra measured at 125, 200 and 250 K. In addition, the data for the conventional PL measurements at 10 K shown in Fig. 3 are included for comparison. For the evaluation of E_{PL} , the maximum of the spectrum was taken. When this was not possible due to fringe patterns in the spectrum, the centre-of-mass was chosen. This gave reliable values because of the symmetry of the spectra. All samples exhibit a similar behaviour, i.e. with increasing SC an increase of E_{PL} is observed. However, the increase seems more pronounced for the PL measurement at 10 K. With increasing temperature, E_{PL} decreases for all samples, in agreement with results in the literature [10].

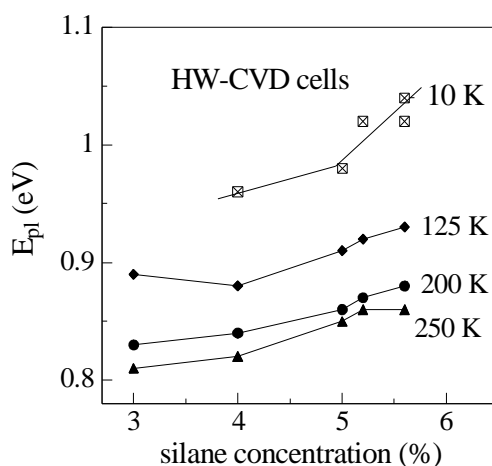


Fig. 5. Photoluminescence peak energy E_{PL} from modulation measurements on solar cells as a function of the silane concentration measured at the indicated temperatures. Data for a conventional PL measurement at 10 K are also shown.

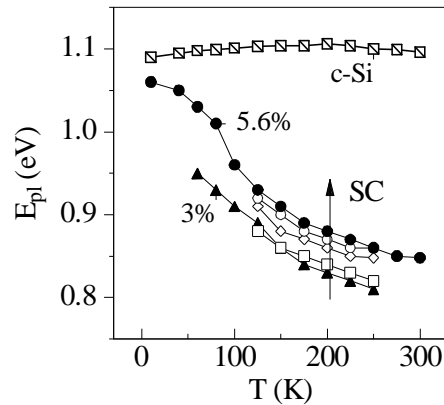


Fig. 6 Photoluminescence peak energy E_{PL} as a function of temperature for the same devices as in Fig. 5.

The dependence of E_{PL} on the measurement temperature for the modulated spectra is shown in Fig. 6 in more detail. Modulated spectra could not be obtained at all temperatures. At low temperatures, the modulation effect decreased strongly for some of the samples. There is strong evidence that this is related to the low mobility of charge carriers, which leads to poor extraction of carriers [15]. At high temperatures, useful results could not be obtained because the low luminescence efficiency causes a poor signal-to-noise ratio. In addition to the results obtained on the microcrystalline solar cells, those obtained on the c-Si photodiode are included in the figure for comparison. It is obvious that all microcrystalline samples exhibit a similar temperature dependence in the investigated temperature range, but the results differ dramatically from the single crystalline case. The c-Si diode has the highest E_{PL} and exhibits only a weak change with temperature, whereas E_{PL} of the microcrystalline solar cell with SC=5.6 %, for example, shows a slightly lower energy at low temperature and decreases strongly with increasing temperature. The increase of E_{PL} with increasing SC, as shown in Fig. 5, is obtained in the whole temperature range.

In Fig. 7, V_{oc} is shown as a function of temperature for the same set of samples as in Fig. 6. These measurements were done under the same conditions as for the modulated PL spectra, and the data have been used as set-points for V_{oc} (compare with Fig. 2). At 10 K, V_{oc} of the c-Si diode is about 1120 mV, and it decreases only weakly below 50 K. At higher temperatures, the decrease is stronger and almost linear with temperature. Similar to the results of the PL measurements shown in Fig. 6, the SC=5.6 % sample exhibits the highest value of all μ c-Si:H solar cells, but the V_{oc} of about 961 mV is significantly lower than that of the c-Si diode. At higher temperatures, the difference of the V_{oc} of c-Si and μ c-Si:H becomes smaller, and at room temperature only a very small difference remains. With decreasing SC, the V_{oc} curves are shifted parallel towards lower values.

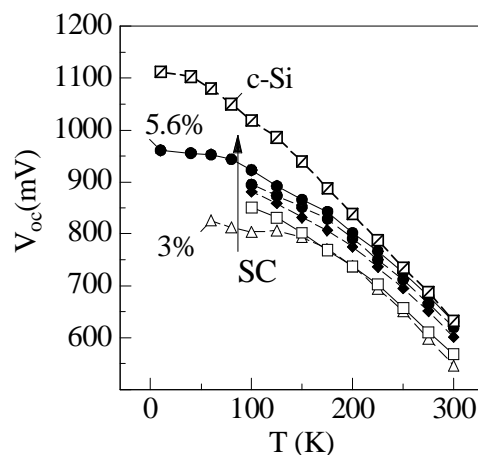


Fig. 7. Open circuit voltage V_{oc} as a function of temperature for the same devices as in Fig. 5.

4. Discussion

As shown in Figs. 1 and 2, an increase in the silane concentration in the gas phase leads to an increase of both the open circuit voltage and the photoluminescence energy. Raman and X-ray diffraction measurements on the same samples reveal a decreasing crystalline volume fraction with increasing SC, e.g. the 'Raman crystallinity', X_c^{RS} [1], decreases from more than 65% for SC=3% to 25% for SC=5.6%. The decrease of the crystallinity is usually accompanied by a broadening of the X-ray diffraction peaks and a decreasing size of the crystalline grain clusters observed in TEM, see e.g. [1] and references therein. This has led to the suggestion of a shift of the band gap of $\mu\text{c-Si:H}$ with decreasing crystallinity, due to quantum size effects, to explain e.g. the shift of E_{PL} [9,11]. We do not consider size effects here, because careful spectral response measurements (not shown) do not reveal a shift of the band edge within experimental error (< 20 meV). Therefore, the increase of almost 100 mV in V_{oc} and E_{PL} with increasing SC requires a different explanation.

A good correlation between the PL peak energy and microstructure, i.e. an increase of the PL energy with decreasing crystalline volume fraction, was previously found for series of undoped $\mu\text{c-Si:H}$ thin films deposited at different substrate temperatures. It was tentatively interpreted as being caused by changes in the density of states distribution due to changes in the microstructure [6]. In the following, we will discuss changes of the density of states distribution as a possible reason for the alteration of both V_{oc} and E_{PL} .

As shown in Figs. 4 and 5, the PL spectrum is broad and featureless and located well below the band gap of c-Si (1.16 eV at 10 K). In agreement with various other experiments that indicate localized states close to the band edges, e.g. [16], the photoluminescence process is attributed to the recombination of electrons and holes in localized states below the conduction band edge and the valence band edge respectively [6]. The energy position and the shape of the PL spectrum are thus determined by the distribution of carriers in these localized states and the transition probabilities for radiative recombination. On the other hand, the distribution of the electrons and holes also determines the V_{oc} in the case of a quasi equilibrium condition, via the splitting of the quasi-Fermi levels of the electrons and holes. Therefore, V_{oc} and E_{PL} are linked via the distribution of the excess carriers. It is therefore expected that both values will exhibit similar trends, but the changes will depend on the details of the density-of-states distribution (DOS). On the other hand, from the investigation of both parameters, information on the DOS can be obtained. It should also be mentioned here that the assumption of the quasi-equilibrium for the photogenerated carriers might not be fulfilled for deep trap states at low temperatures. It is not clear how these conditions could be described appropriately.

When compared to c-Si, the V_{oc} of the $\mu\text{c-Si:H}$ cells is lower at all temperatures but the difference is largest at low temperatures and becomes smaller at high temperatures. At low temperatures, the Fermi-Dirac distribution is sharp and the quasi-Fermi-level splitting is determined by the integration over the DOS up to the quasi-Fermi-level. The smaller splitting of the quasi-Fermi-level in the $\mu\text{c-Si:H}$ cells is therefore strong evidence for a high DOS below the band gap in these cells. These states shall be identified with the localized band tail states evidenced by other techniques, e.g. [16, 17]. The much larger width of the PL band of the $\mu\text{c-Si:H}$ films and solar cells compared to their crystalline counterpart strongly supports this interpretation. Also the temperature dependence of E_{PL} is in line with this interpretation. The results can be discussed based on the well-accepted model for radiative recombination between localized states in a-Si:H (see e.g. [13]), where the temperature dependent shift of E_{PL} is caused by a superposition of the shift of the optical gap and the shift of the carrier distribution to lower energies. The latter is due to competing non-radiative recombination processes.

The increase of E_{PL} and V_{oc} with increasing SC at a given temperature is interpreted by a reduction of the density of band tail states. This results in a shift of the carrier distributions to higher energy, and thus to a shift of the photoluminescence spectra to higher energies and to a larger splitting of the quasi-Fermi levels, i.e. an increase of V_{oc} , if the carrier concentration remains almost constant. As shown in Fig. 4, the photoluminescence intensity does not change significantly, and therefore the quantum efficiency remains fairly constant. Changes in the defect concentration can therefore be ruled out, and the assumption of a constant carrier concentration seems appropriate. Investigations of the short circuit current density j_{sc} on the solar cells studied here reveal a decreases

of j_{sc} , i.e. a decreasing carrier collection, with decreasing temperature below about 200 K [15]. In contrast, j_{sc} of the c-Si solar cell remains almost constant down to 50 K whereas j_{sc} of an a-Si:H solar cell already starts to drop below 250 K. This indicates a decreasing carrier drift length in μ c-Si:H, probably due to a decreasing carrier mobility towards low temperature in agreement with results from Hall measurements on μ c-Si:H films which have been interpreted as evidence for tail states [17]. Further support for the interpretation presented here stems from model calculations of PL spectra for a given DOS and quasi-Fermi level splitting, i.e. V_{oc} (see [18]), and from the results of V_{oc} as a function of the generation rate [15]. The results are consistent with the assumption that band tail states act as traps for photogenerated carriers and limit the shift of the quasi-Fermi levels towards higher energies.

Although there is only little known on the cause of the band tail states on a microscopic scale, strain and interface states at the crystalline grains are possible sources for such states. We propose that the reduction of the density of band tail states is due to structural relaxation of the μ c-Si:H network by the incorporation of hydrogen or amorphous hydrogenated silicon. This effect would be similar to that obtained in polycrystalline-silicon thin film transistors, where a significant reduction in the concentration of tail states has been observed after hydrogenation [19].

5. Conclusions

The change of E_{PL} , and V_{oc} , in μ c-Si:H solar cells, as a function of the silane concentration and temperature, can be interpreted assuming band tail states extending from the band edges into the band gap of silicon. The decrease of E_{PL} and V_{oc} with increasing temperature is due to the change of the carrier distributions in the band tails, and the accompanying shift of the quasi-Fermi energies to lower energies. The increase of E_{PL} and V_{oc} for increasing SC is attributed to a reduced density of band tail states. It is suggested that hydrogen or hydrogenated amorphous silicon surrounding the crystalline phase leads to an improved lattice relaxation, and that thereby the density of band tail states is reduced. The differences between HW-CVD and PE-CVD material and solar cells shall be explored by a similar study.

Acknowledgements

We gratefully acknowledge technical support by M. Hülsbeck, J. Wolf and S. Michel, and financial support by the Bundesministerium für Umwelt, Naturschutz und Reaktorsicherheit under contract no. 0329814A.

References

- [1] L. Houben, M. Luysberg, P. Hapke, R. Carius, F. Finger, H. Wagner, *Phil. Mag. A* **77**, 1447 (1998).
- [2] O. Vetterl, F. Finger, R. Carius, P. Hapke, L. Houben, O. Kluth, A. Lambertz, A. Mück, B. Rech, H. Wagner, *Solar Energy Materials and Solar Cells* **62**, 97 (2000).
- [3] J. Meier, E. Vallat-Sauvain, S. Dubail, U. Kroll, J. Dubail, S. Golay, L. Feitknecht, P. Torres, S. Fay, D. Fischer, A. Shah, *Solar Energy Materials and Solar Cells* **66**, 73 (2000).
- [4] O. Vetterl, R. Carius, L. Houben, C. Scholten, M. Luysberg, A. Lambertz, F. Finger, H. Wagner, *Mater. Res. Soc. Symp. Proc.* **609**, A15.2 (2000).
- [5] S. Klein, F. Finger, R. Carius, B. Rech, L. Houben, M. Luysberg, M. Stutzmann, *Mater. Res. Soc. Symp. Proc.* **715**, A26.2 (2002).
- [6] R. Carius, T. Merdzhanova, F. Finger, S. Klein, O. Vetterl, *J. Materials Science: Materials in Electronics* **14**, 625 (2003).
- [7] R. Carius, T. Merdzhanova, F. Finger, *Mater. Res. Soc. Symp. Proc.* **762**, A4.2 (2003).
- [8] R. Carius, F. Finger, U. Backhausen, M. Luysberg, P. Hapke, H. Overhof, *Mater. Res. Soc. Symp. Proc.* **467**, 283 (1997).

- [9] D. Han, G. Yue, J. D. Lorentzen, J. Lin, H. Habuchi, Q. Wang, *J. Appl. Phys.* **87**, 1882 (2000).
- [10] G. Yue, J. D. Lorentzen, J. Lin, D. Han, Q. Wang, *J. Appl. Phys.* **88**, 4904 (2000).
- [11] A. Kaan Kalkan, S. J. Fonash, Shang-Cong Cheng, *Appl. Phys. Lett.* **77**, 55 (2000).
- [12] P. K. Bhat, G. Diprose, T. M. Searle, I. G. Austin, P. G. LeComber, W. E. Spear, *Physica B* **117 - 118**, 917 (1983).
- [13] R. A. Street, *Adv. Phys.* **30**, 593 (1981).
- [14] S. Klein, F. Finger, R. Carius, T. Dylla, B. Rech, M. Grimm, L. Houben, M. Stutzmann, *Thin Solid Films* **430**, 202 (2003).
- [15] T. Merdzhanova, R. Carius, F. Finger, S. Klein, D. Dimova-Malinovska, *Thin Solid Films* **451 - 452**, 285 (2004).
- [16] S. Reynolds, V. Smirnov, C. Main, R. Carius, F. Finger, *Mater. Res. Soc. Symp. Proc.* **762**, A3.4.1 (2003).
- [17] R. Carius, J. Müller, F. Finger, N. Harder, P. Hapke in *Thin Film Materials and Devices – Developments in Science and Technology*, eds. J.M. Marshall, N. Kirov, A. Vavrek, J. M. Maud, (World Scientific Publishing Co.), p. 157 (1999).
- [18] T. Merdzhanova, R. Carius, F. Finger, S. Klein, D. Dimova-Malinovska, *J. Optoelectron. Adv. Mater.* **7**(1), 485 (2005).
- [19] J. R. Ayres, *J. Appl. Phys.* **74**, 1787 (1993).